Neuron, Volume *59*

Supplemental Data

Localized Regulation of Axonal RanGTPase Controls Retrograde Injury Signaling in Peripheral Nerve

Dmitry Yudin, Shlomit Hanz, Soonmoon Yoo, Elena Iavnilovitch, Dianna Willis, Tal Gradus, Deepika Vuppalanchi, Yael Segal-Ruder, Keren Ben-Yaakov, Miki Hieda, Yoshihiro Yoneda, Jeffery L. Twiss, and Mike Fainzilber

Figure S1. Schematic of Nucleocytoplasmic Transport
The gradient of RanGTP in the nucleus versus RanGDP in the cytoplasm is defined by the strict nuclear localization of RCC1, the sole known RanGEF, and the occurrence of RanBP1 and RanGAP, the RanGTP displacing and hydrolyzing facilitators, in the perinuclear zone of the cytoplasm. RanGTP exits the nucleus in complex with importin β or with CAS and importin α, and encounters RanBP1 and RanGAP, which catalyze its dissociation and hydrolysis to the GDP-bound form. The importins are then free to associate with each other to form a high affinity carrier for NLS-containing cargo proteins for import to the nucleus.

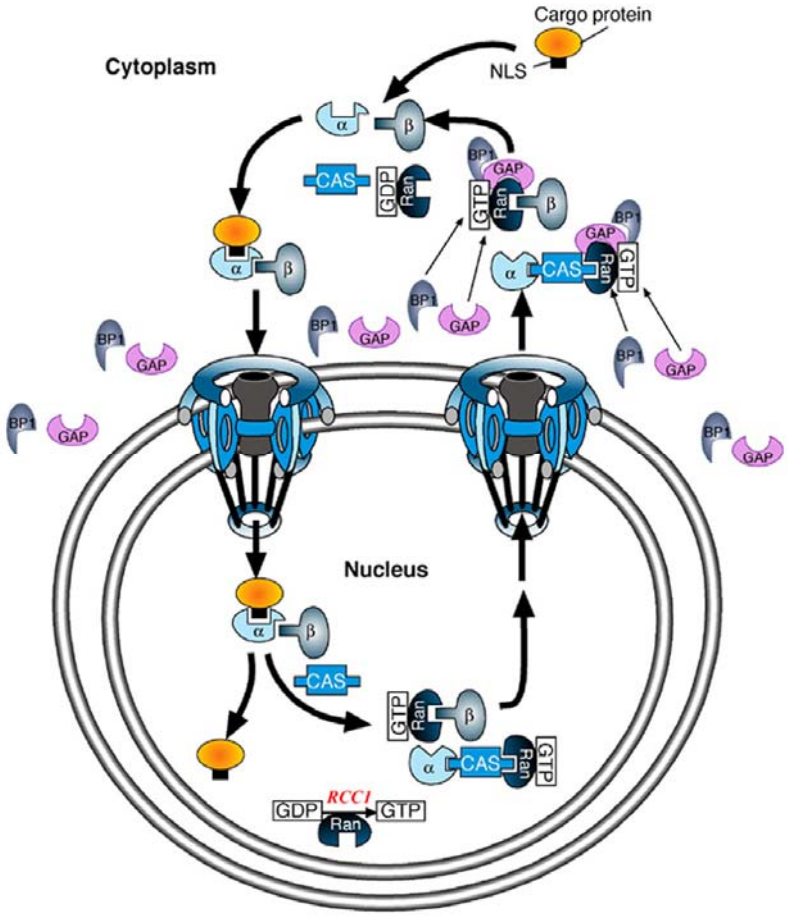

Figure S2. RCC1 Is Not Found in Sciatic Nerve Axons

(**A**) Western blot analysis for RCC1 and the glial marker GFAP in brain extract compared with sciatic nerve axoplasm taken at the indicated times (hr) after injury. 40 μg protein per lane. (**B**) Immunostaining for RCC1 compared with the axon marker NF-H in cultured DRG neurons. (**C**) Immunostaining for RCC1 versus NF-H on cross-sections of sciatic nerve after lesion. All images were taken at x60 magnification.

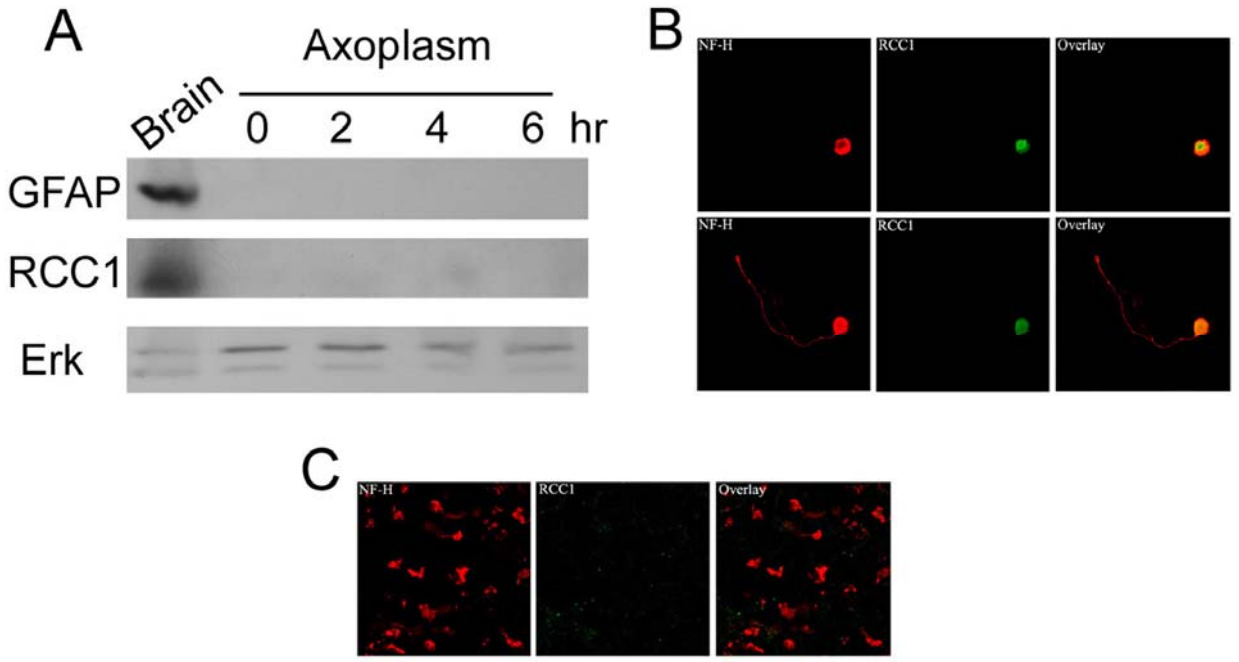

Figure S3. Endogenous RanBP1 mRNA in DRG Axons

RanBP1 mRNA is found in neurofilament positive axons in cultured injury-conditioned DRGs. **(A)** Cultures of injury-conditioned DRGs were stained for neurofilament protein (green) and hybridized for RanBP1 mRNA (red). The image displays a three-dimensional projection of 15 optical XY planes taken at ~ 0.2 μm intervals. **(B)** The same image as in A, showing only the RanBP1 mRNA signal. Notice that the RanBP1 signal is granular in nature and is clearly observed in the axons (arrows), as well as in adjacent the Schwann cells (arrowhead). **(C)** A high magnification confocal image of cultures stained for neurofilament protein (green) and RanBP1 mRNA (red). The panel shows a single optical XY plane of a segment of a distal axon. **(D)** The same image as in C shows that the RanBP1 mRNA signal is coarsely granular and extends the length of the distal axon. (**E)** RNA FISH for β-actin mRNA shows a similar granular pattern to the signal observed for RanBP1. The inset panel shows the corresponding neurofilament signal for this axon. **(F)** RNA FISH using a scrambled probe to demonstrate the specificity of the RanBP signal. Only weak background is observed, with no granular signal detected. The inset shows the corresponding neurofilament signal. All images in C-F are confocal images of single optical XY planes with matched exposure levels.

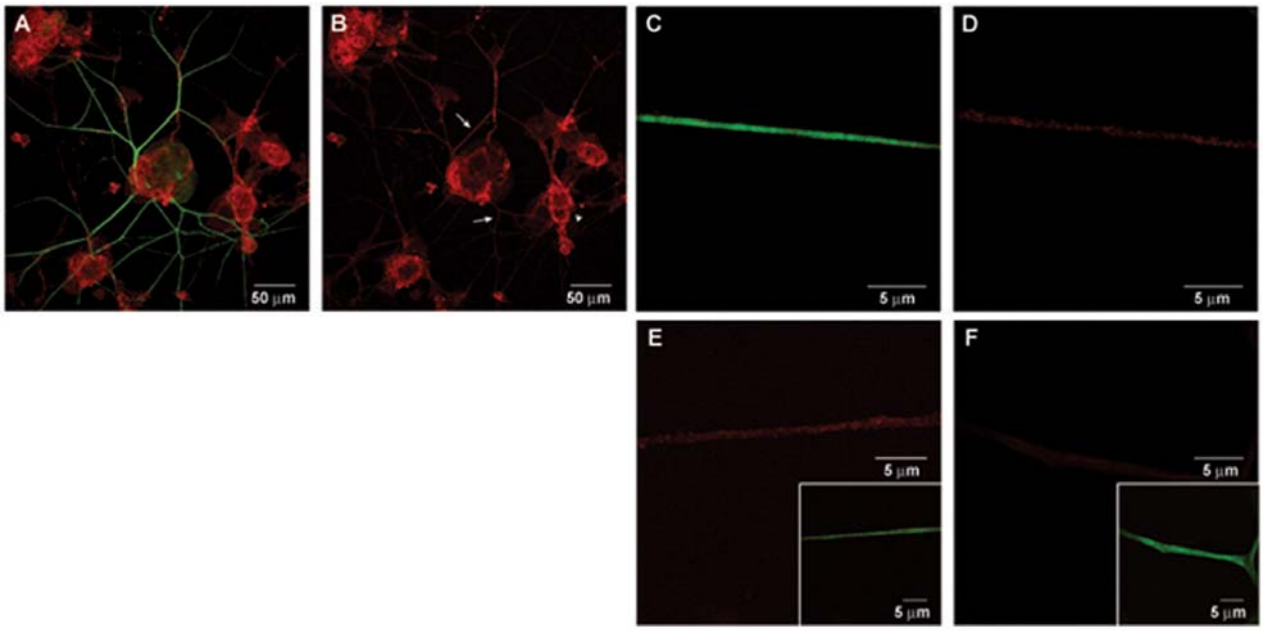

Figure S4. Cloning of RanBP1 3'UTR Variants

Nested PCR was performed on axoplasm cDNA obtained from non-injured (N) and injured (I, 18 hr post-lesion) sciatic nerve ("Axon"). Comparative reactions were performed on cDNA prepared from the corresponding DRG ganglia ("Soma"). Two forward primers were designed at the end of ORF (5'-CGAGTGTCCCAAGCCTGA-3' for the first reaction, 5'- CAGAGACGAGGCTGAAGA-3' for the second reaction) and polyT reverse primer (5'-GACCACGCGTATCGATGTCGACTTTTTTTTTTTTTTT-3'). Both PCR reactions were conducted for 40 cycles, 1 min each step. PCR products were run on agarose gel, extracted from the gel and cloned into EcoRI and SalI sites of pEGFP-C1 plasmid (Clonech). (**A**) Gel images of products from representative reactions. (**B, C**) Sequences of the two main products, comprising the shared 3' region of the open reading frame and the long or short UTR.

A

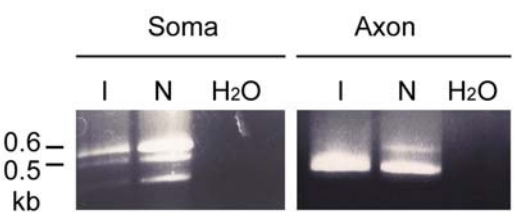

B

Ran BP1 Short 3'UTR (Genbank Accession # EU146304)

```
tcagagacga ggctgaagag aagtctgagg agaagcaatg aatcattctg
tctttttcct ttccttttct ttttaaaaat ttgccccacc ctttaaggtt
tgtttttatt ctgttttgtt tttacaaggg actttataaa gaactgaatt
ccaaaaaaaa aaaaaaaaa
```

C

Ran BP1 Long 3'UTR (Genbank Accession # EU146305)

```
cagagacgag gctgaagaga agtctgagga gaagcaatga atcattctgt
cttttttcctt tccttttctt tttaaaaatt tgccccaccc tttaaggttt
gtttttattc tgttttgttt ttacaaggga ctttataaag aactgaattc
caaccttcag gttgtctttt ttttttttt aacttttttt tttcctccaa
gttttgacac cattgaacat gacttcagaa atccattccc cagtcatgaa
aatgtactgt gctaactttc ttttccatag tggaaacact tatttatagt
catcaaaaat agtgaataaa aaatgccttt gaaaacctga aaaaaaaaaa
aaaaaaa
```

Figure S5. FRAP Analyses in DRG Neurons

Representative images from time-lapse sequences before (-4 min) and after photobleaching (series from 0 to 20 min) of adult DRG neurons transfected with 3' UTR constructs fused to destabilized GFP. L, long UT variant, S, short UTR variant, Δ, differential segment from the distal part of the long UTR., anis. indicates transfected neurons that were treated with 1 μM anisomycin immediately prior to pre-bleach imaging. The boxed regions represent the area subjected to photobleaching with recovery monitored over 20 min. Representative recordings of the complete time range are shown in supplemental movies 1-5. Scale bars are 50 μm.

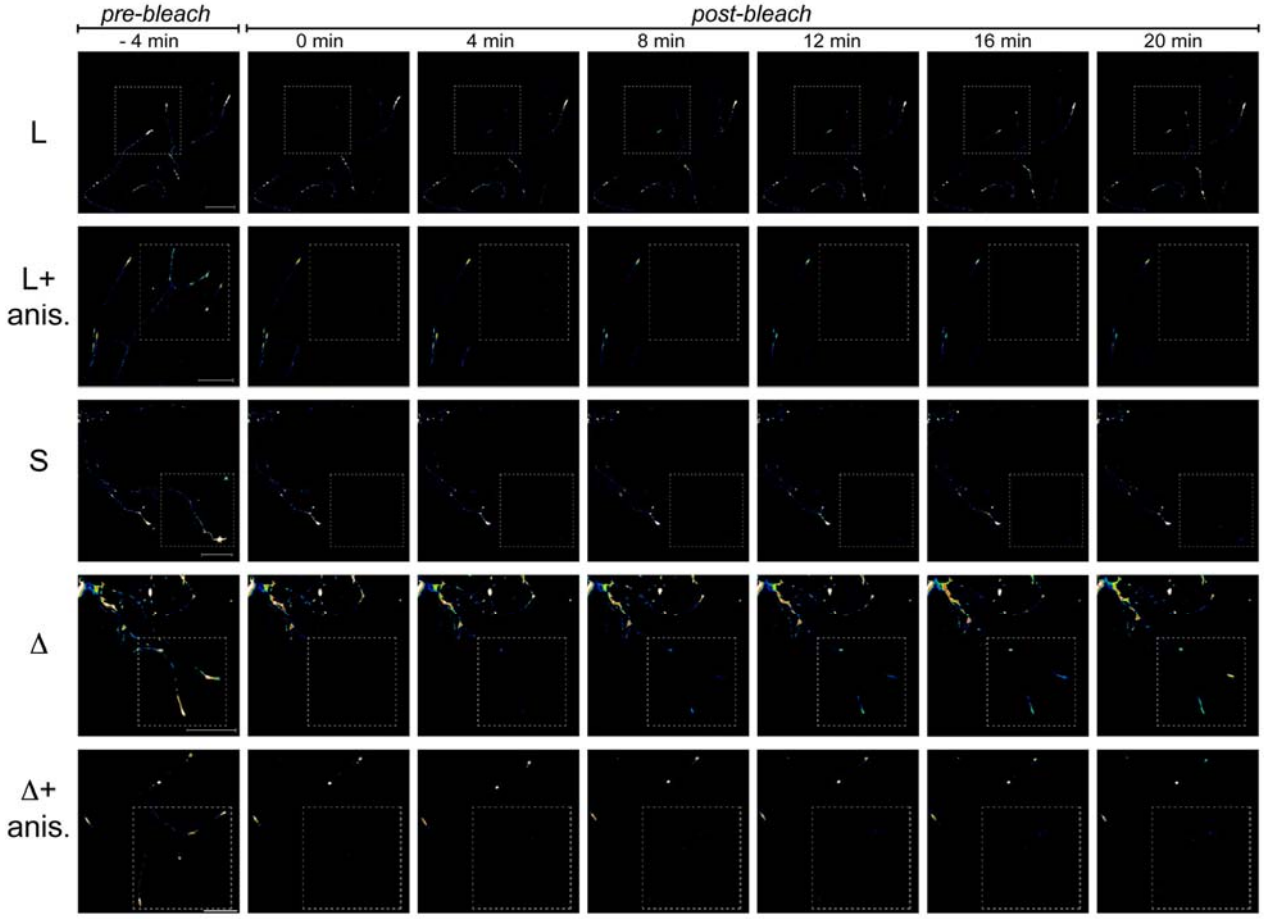

Figure S6. FRAP Analyses of myr-dzGFP-3'UTR-RanBP1 Compared to Kif5c-dTomato

(A) Fluorescence intensity over multiple time-lapse sequences of myr-dz-GFP-3'UTR-RanBP1 compared to Kif5c-dTomato. Average recoveries (% of pre-bleach levels) ± SEM are shown for both constructs (n = 5 for RanBP1 and 3 for Kif5c). A two-ANOVA with post-hoc test was employed to test statistical significance of recovery of myr-dz-GFP-3'UTR-RanBP1 at each time point vs. 0 min post-bleach (* $p<0.05$, ** $p<0.01$, *** $p<0.001$) and in comparison to Kif5c-dTomato (†† $p<0.01$, ††† $p<0.001$). **(B)** Representative images from time-lapse sequences of a double photobleach experiment. Top shows an adult DRG neuron transfected with myr-dz-GFP fused to the long RanbP1 3'UTR with the bleached regions indicated. The more distal region was subjected to a single round of bleaching while the more proximal region was repetitively bleached. Scale bar is 25 µm. Recovery in both the distal and proximal regions was monitored over 20 min (See also supplemental movie). An arrow indicates the growth cone. **(C)** Fluorescence intensity over multiple time-lapse sequences of myr-dz-GFP-3'UTR-RanBP1 compared to Kif5c-dTomato of double photobleach experiments. Average recovery (normalized to time 0) ± SEM is shown for both the distal and proximal regions (n = 4-6).

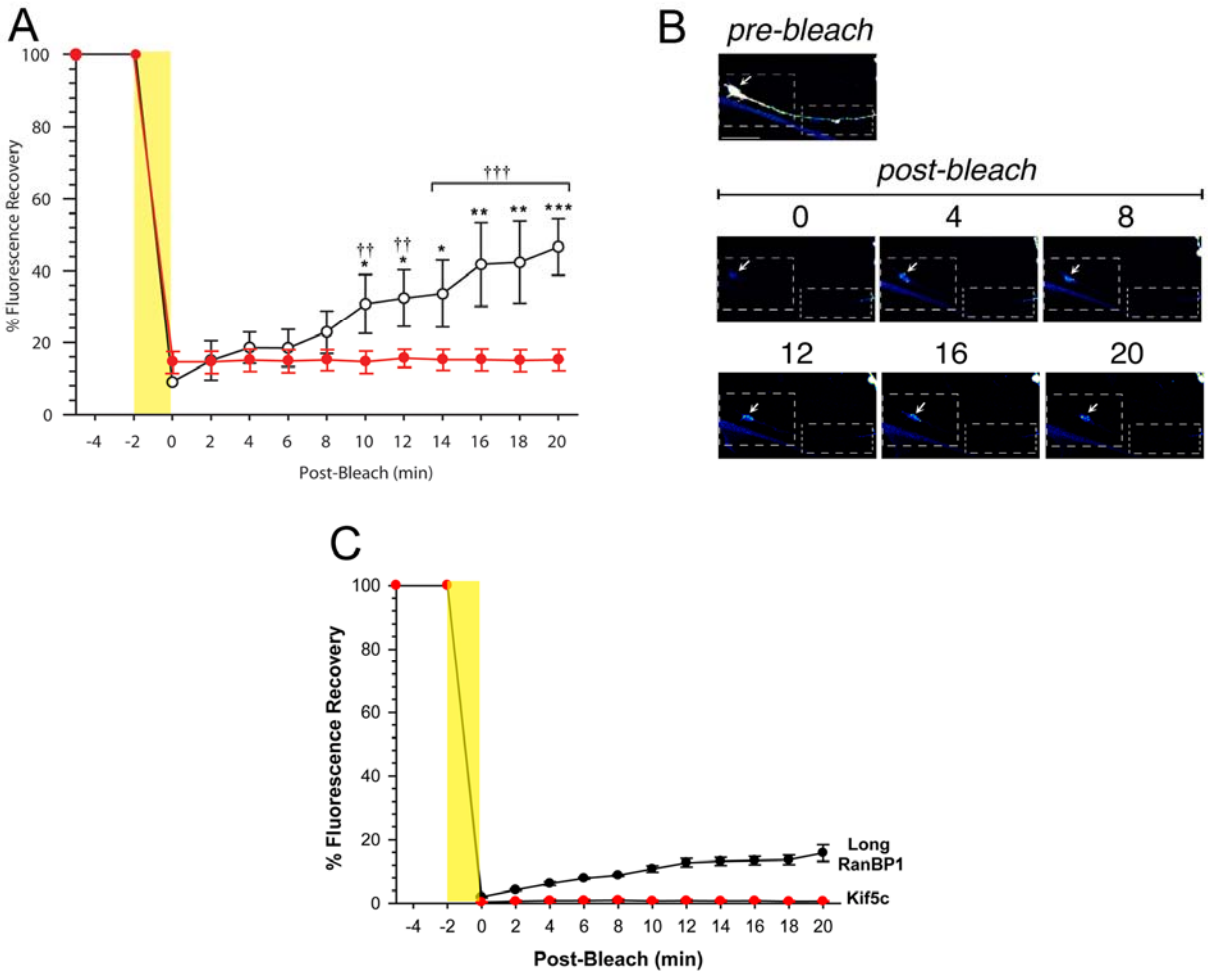

Figure S7. Uptake and Stability of Exogenous Proteins in Sciatic Nerve Axons after Injury

(**A**) Representative images of streptavidin-Alexa Fluor 647 (green) injection to lesioned sciatic nerve and uptake into NFH-positive (red) axons, monitored by confocal microscopy on cross-sections immediately proximal to the lesion and injection site. Time points shown are 0, 3 and 6 hours after crush lesion concomitant with injection of 20 µg fluorescent streptavidin (Molecular Probes Catalog # S32357). (**B**) Quantification of the fraction of axons containing streptavidin at the indicated time points (average ± standard deviation, n = 3). (**C**) Levels of injected RanQ69L protein in axoplasm. 32 µg of His-tagged RanQ69L were injected into sciatic nerve in vivo concomitantly with crush lesion, and axoplasm was extracted from the injected nerves at the indicated time points. His-tagged protein was purified over Nickel-NTA agarose, and detected by Western Blot. Erk served as an input loading control. (**D**) Densitometric quantification of the levels of RanQ69L in axoplasm at the indicated time points (average ± standard deviation, n = 3).